

# 10-Gingerol Enhances the Effect of Taxol in Triple-Negative Breast Cancer via Targeting ADRB2 Signaling

Yuqi Liang<sup>1,2,\*</sup>, Guosong Wu<sup>3,\*</sup>, Tianyu Luo<sup>1,2,\*</sup>, Haimei Xie<sup>2</sup>, Qian Zuo<sup>2</sup>, Ping Huang<sup>2</sup>, Huachao Li<sup>2</sup>, Liushan Chen<sup>2</sup>, Hai Lu<sup>4,\*</sup>, Qianjun Chen<sup>1,2,\*</sup>

<sup>1</sup>The Second Clinical College of Guangzhou University of Chinese Medicine, Guangzhou, Guangdong, 510006, People's Republic of China;

<sup>2</sup>Department of Breast, Guangdong Provincial Hospital of Chinese Medicine, Guangzhou, Guangdong, 510120, People's Republic of China; <sup>3</sup>Nanfang Hospital Baiyun Branch, Guangzhou, Guangdong, 510000, People's Republic of China; <sup>4</sup>The First People's Hospital of Shaoguan, Shaoguan, Guangdong, 512099, People's Republic of China

\*These authors contributed equally to this work

Correspondence: Qianjun Chen, Department of Breast, Guangdong Provincial Hospital of Chinese Medicine, 111 Dade Road, Yuexiu District, Guangzhou, 510102, People's Republic of China, Email [cqj55@163.com](mailto:cqj55@163.com); Hai Lu, The First People's Hospital of Shaoguan, No. 3, South Dongdi Road, Shaoguan, 512099, People's Republic of China, Tel +86 15622187291, Email [hysa1985@163.com](mailto:hysa1985@163.com)

**Purpose:** Although paclitaxel is widely used in cancer treatment, severe side effects and drug resistance limit its clinical use. 10-gingerol (10-G) is a natural compound isolated from ginger, which displays anti-inflammatory, antioxidant, and antiproliferative properties. However, the chemotherapy-sensitization effect of 10-G on triple-negative breast cancer (TNBC) has not been fully clarified. This study is aimed at investigating the effect of 10-G on the paclitaxel sensitivity in TNBC, and its underlying mechanism.

**Methods:** The study was determined through in vitro and in vivo experiments. Cell viability and proliferation were detected by cell counting kit 8 (CCK-8) and colony formation. To detect cell apoptosis, flow cytometry and TUNEL were used. The expression of proteins was detected by Western blotting and immunohistochemistry. The molecular docking and gene knockout were corroborated by interactions between 10-G and adrenoceptor Beta 2 (ADRB2). The body weight of mice, histopathology and organs (kidney and spleen) coefficients were used to monitor the drug toxicities.

**Results:** In vitro, 10-G increased the sensitivity of TNBC cells to paclitaxel, and could synergistically promote the apoptosis of TNBC cells induced by paclitaxel. In combination with molecular docking and lentivirus knockdown studies, ADRB2 was identified as a 10-G binding protein. 10-G inhibited ADRB2 by binding to the active site of ADRB2. Knockdown of ADRB2 reduces the proliferation activity of TNBC cells but also attenuates the sensitizing effects of 10-G to paclitaxel. Western blotting and immunohistochemistry showed that 10-G played an anti-proliferation and chemotherapy-sensitizing role by inhibiting the ADRB2/ERK signal. Toxicity evaluation showed that 10-G would not increase hepatorenal toxicity with paclitaxel.

**Conclusion:** This data suggests that 10-G may be used as a new chemotherapeutic synergist in combination with paclitaxel to enhance anticancer activity. The potential value of ADRB2 as a target for improving chemotherapy sensitivity was also emphasized.

**Keywords:** triple-negative breast cancer, combined therapies, 10-gingerol, paclitaxel, adrenoceptor Beta 2

## Introduction

Breast cancer is the most commonly diagnosed and the leading cause of cancer death among women worldwide.<sup>1</sup> Breast cancer without expression of ER, PR, and HER2 is termed triple-negative breast cancer (TNBC) and is the most aggressive type.<sup>2</sup> It has the clinical characteristics of high recurrence and mortality rates.<sup>3</sup> Since no effective therapeutic target currently exists, chemotherapy remains the main treatment option for TNBC.<sup>4</sup> Paclitaxel, which effectively eradicates tumor cells, is still considered the first-line anticancer drug in numerous human cancers including TNBC.<sup>5</sup> However, the resistance of cancer cells to paclitaxel seriously hinders its clinical application.<sup>6</sup> Thus, it is urgent to

develop more effective and safer anti-cancer drugs, which can improve the inhibitory effect of chemotherapy drugs on TNBC, thereby improving prognosis.

A large number of studies have shown that some natural plant extracts and bioactive phytochemicals can improve the effectiveness of chemotherapy.<sup>7-9</sup> Among such plant-natural products is ginger, which is widely used as a flavoring and dietary supplement.<sup>10</sup> 10-gingerol (10-G) is the principal pungent compound of ginger, which has anti-inflammatory, antioxidant, and antiproliferative properties.<sup>11</sup> Studies show that compared with other gingerol compounds in ginger, 10-G has the highest anti-tumor activity and can induce apoptosis in a variety of malignant tumor cells, including breast cancer.<sup>12,13</sup> As a safe natural compound, 10-G improves the anti-cancer activity of anthracycline doxorubicin in TNBC.<sup>14</sup> No published study has, however, demonstrated the effect and underlying molecular mechanisms of 10-G on the efficacy of paclitaxel in TNBC so far.

Based on network pharmacology analysis, adrenoceptor Beta 2 (ADRB2) is a potential target for 10-G inhibition of TNBC.<sup>15</sup> ADRB2, which belongs to the G protein-coupled receptor (GPCR) superfamily as the encoding gene of the  $\beta_2$ -adrenergic receptor, is involved in the development of a variety of malignant tumors.<sup>16,17</sup> Studies show that ADRB2 is a potential target for improving the sensitivity of chemotherapy and the clinical prognosis of various malignancies.<sup>18,19</sup> The use of ADRB2 blockers reduces the risk of breast cancer metastasis and recurrence.<sup>20,21</sup> A study in hepatocellular carcinoma showed that silencing increased the antitumor activity of sorafenib.<sup>22</sup> Targeting ADRB2 may be a novel strategy for enhancing the therapeutic efficacy of paclitaxel in TNBC.

This study shows that 10-G potentiates the effect of paclitaxel on TNBC. ADRB2 is a major target in the therapy of 10-G, while the effect of 10-G in enhancing paclitaxel was linked to ADRB2/ERK signaling. In vivo and in vitro experiments showed that 10-G had no obvious toxic and side effects on mammary epithelial cells and mouse organs. This result not only provides a mechanistic explanation for the anticancer activity of 10-G but also provides an opportunity to develop chemotherapeutic synergistic drug therapy for TNBC.

## Material and Methods

### Reagents and Antibodies

The following antibodies were used: Bcl-2 (ABCAM, Cambridge, UK, ab182858), Bax (Cell Signaling Technology, Danvers, MA, 2772); cleaved-PARP (Cell Signaling Technology, Danvers, MA, 5625), ADRB2 (Proteintech, Wuhan, China, 13096-1-AP), ERK (ABCAM, Cambridge, UK, ab17942), phospho-ERK1/2 (ABCAM, Cambridge, UK, ab201015), Ki67 (ABCAM, Cambridge, UK, ab16667) and  $\beta$ -actin (Proteintech, Wuhan, China, 66009-1-Ig), horseradish peroxidase (HRP)-conjugated goat anti-rabbit (Proteintech, Wuhan, China, SA00001-2), horseradish peroxidase (HRP)-conjugated goat anti-mouse (Proteintech, Wuhan, China, SA00001-1). 10-G was purchased from Chengdu Ruifensi Biotechnology Co., Ltd. (Chengdu, China), and a stock solution of 40 mM was dissolved in dimethyl sulfoxide (Sigma-Aldrich; Merck KGaA). Its molecular formula is C<sub>21</sub>H<sub>34</sub>O<sub>4</sub>, and its structural formula is depicted in Figure 1. Paclitaxel injection was obtained from Hainan Quanxing Pharmaceutical Co., Ltd.

### Cell Culture

Human TNBC cell lines MDA-MB-231 and SUM-159 and non-tumor breast epithelial cell MCF-10A were purchased from the American Type Culture Collection (ATCC, Manassas, VA). The TNBC cells (MDA-MB-231 and SUM-159) were cultured at 37°C with 5% carbon dioxide in medium (MDA-MB-231: DMEM medium and SUM-159: RPMI 1640 medium) supplemented with 10% fetal bovine serum and 100 U/mL penicillin and 100  $\mu$ g/mL streptomycin solution

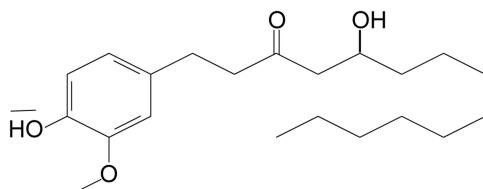


**Figure 1** The structural formula of 10-G.

(Gibco Life Technologies, Lofer, Austria). MCF-10A was cultured in Dulbecco's modified Eagle medium containing 5% horse serum, 100 U/mL penicillin, and 100 µg/mL streptomycin solution (Gibco Life Technologies, Gaithersburg, MD), 20 ng/mL recombinant human epidermal growth factor, 0.5 µg/mL hydrocortisone, 100 ng/mL cholera toxin and 10 µg/mL insulin (Sigma-Aldrich, Shanghai, China).

## Cell Viability and Combined Effect Analysis

Cells were collected and seeded in 96-well plates at a density of 2000 cells/well for 12 h. The cells were cultured in different concentrations of 10-G (0, 25, 50, 100, 150, 200, 400 and 800 µM) and/or paclitaxel (0, 25, 50, 100, 200, 400, 800 and 1600 nM) for 48 h, after which 10 µL of Cell Counting Kit-8 solution was added to each well. The optical density (OD) was calculated at 450 nm using a microplate reader (Bio-Rad Model550, CA) after 4 h. The combined index (CI) was calculated using Compusyn (Computusyn, Inc.) software. The analysis generally defines CI values of 0.9–1.1 as additive, 0.3–0.9 as synergistic, and <0.3 as strongly synergistic, whereas values >1.1 are considered as antagonistic. The median inhibitory concentration (IC<sub>50</sub>) was obtained by Prism 8 (GraphPad software).

## Colony Formation Assay

For the colony formation assay, 800 cells were incubated in six-well plates. After 24 h culture at 37°C, the cells were then disposed with 10-G (100 µM) and/or paclitaxel (100 nM) in a medium containing 10% FBS for 14 days. The plates were stained with crystal violet (Beyotime, Jiangsu, China) for 20 min after fixing with 4% paraformaldehyde for 60 min. After washing with PBS for 10 min, the colonies were counted using ImageJ (ImageJ 1.53e, Maryland, USA) software when the cells were air-dried.

## Cell Apoptosis Analysis

Flow cytometry and annexin V-FITC/PI apoptosis detection kit (Beyotime, Jiangsu, China) were used. About  $2 \times 10^5$  cells were shared equally among the six-well plates. During the exponential phase of cell growth, the cells were exposed to indicated doses of 10-G and paclitaxel individually or in a combination for 24 h. Annexin V-FITC/PI staining was performed according to the manufacturer's instructions (Beyotime, Jiangsu, China). As a percentage of the total cell count, NovoExpress 1.4.1 software (ACEA Bioscience, Inc.; Agilent Technologies, Inc.) was used to estimate the subpopulations of early and late apoptotic as well as dead cells. Cells with annexin V-FITC but negative for PI were considered an early-stage apoptosis subpopulation. Cells positive for both annexin V-FITC and PI were assessed for late-stage apoptosis. Cells with PI but negative for annexin V-FITC were considered dead cells. The cell apoptosis rate is the percentage of the sum of early and late-stage apoptosis. The data presented represent an average of three independent experiments.

## Western Blotting Analysis

MDA-MB-231 and SUM-159 cells at the logarithmic growth stage were divided into control group, 10-G (50 µmol) group, 10-G (100 µmol) group, paclitaxel group, paclitaxel and 10-G (50 µmol) group, and paclitaxel and 10-G (100 µmol) group. About  $2 \times 10^5$  cells were inoculated into six-well plates. After 24 h, the original medium was abandoned, the control group was given an equal volume of complete medium, and other groups were added with Medicated medium: 10-G (50 µmol/L), 10-G (100 µmol/L), paclitaxel (100 nmol/L), paclitaxel (100 nmol/L)+10-G (50 µmol/L) and paclitaxel (100 nmol/L)+10-G (100 µmol/L), respectively. Cells were collected 24 h after treatment, lysed with a radioimmunoprecipitation assay (RIPA) buffer (Sigma-Aldrich, St. Louis, MO), and the supernatant solution was collected. Total protein concentration was measured using the BCA kit (Beyotime, Jiangsu, China). Western blotting was also performed using standard methods.<sup>23</sup> After protein denaturation, 20 µg of extracted protein was fractionated on a 10% SDS-PAGE gel and then transferred to a polyvinylidene fluoride (PVDF) membrane with a 0.45-mm pore size (Millipore, MA, USA). The membranes were then blocked in 5% milk at room temperature for 1 h, washed by TBST (Beyotime, Jiangsu, China) and incubated overnight on a shaker at 4°C for the primary antibody. The primary antibody concentrations were as follows: Bcl-2 (1:1000), Bax (1:1000); cleaved-PARP (1:1000), ADRB2 (1:1000), ERK (1:1000), phospho-ERK1/2 (1:1000), and β-actin (1:1000). ERK and β-actin were used as a loading control. After three washes

with TBST, horseradish peroxidase (HRP)-conjugated goat anti-rabbit (1:5000) and rabbit anti-mouse (1:5000) were used as secondary antibodies and were incubated at room temperature for 1 h. ECL (Tanon Science & Technology, Shanghai, China) was used for color rendering. Band intensity was visualized using ChemiDoc TMXRS+ (Bio-RAD, USA). ImageJ (ImageJ 1.53e, Maryland, USA) software was used to calculate the gray values of each band.

## Establishment of Stable ADRB2-shRNA Cell Lines

The stable ADRB2 knockdown cells were generated via transfecting lentivirus of ADRB2-shRNA (Table 1). ADRB2-shRNA lentiviruses were purchased from Shanghai Gikegen Technology Co., LTD. About  $2 \times 10^5$  cells (MDA-MB-231 and SUM-159) were seeded into each well of the 6-well plate with a total volume of 1 mL medium, and the cells were incubated overnight. Stable ADRB2 knockdown MDA-MB-231 and SUM-159 cell lines were produced by infecting lentivirus (MOI 50 and 20, respectively) and selection with 1 mg/mL puromycin for about 1 week. Western blotting was then used to verify stable cell lines.

## Molecular Docking

The ChemDraw Professional 15.1 software was used to plot the 10-G molecular formula (PerkinElmer, USA). The crystal structure of ADRB2 (PDB Code:3NYA) was obtained from the RSCB protein data bank (<https://www.rcsb.org/>). The docking simulation<sup>24</sup> was performed using the Accelrys Discovery Studio 3.5 (Accelrys, Inc., USA).

## Breast Cancer Xenografts in NOD/SCID Mice

Twenty female NOD/SCID mice, five-week-old, and weighing  $19 \pm 0.5$ g were obtained from the Experimental Animal Centre of Southern Medical University. All mice were housed in cages (five mice per cage) under pathogen-free conditions at 25 °C, 40–60% relative humidity, and 12-h light/dark cycle in the experimental animal center of Guangdong Provincial Hospital of Chinese Medicine. All mice had ad libitum access to standard rodent chow and filtered water and were acclimatized for 1 week before the initiation of the experiment. The use of laboratory animals was checked by the Institutional Animal Ethical Committee (IAEC), and all procedures were approved by the Ethics Committee of Guangdong Provincial Hospital of Chinese Medicine (Reference No. 2020031) and performed according to the Principles of Laboratory Animal Care as well as specific national laws where applicable. All experimental protocols and handling of the animals followed the Guide for the Care and Use of Laboratory Animals (Institute of Laboratory Animal Research, 2011. Guide for the care and use of laboratory animals. Washington (DC): National Academies Press).

For a xenograft model, human MDA-MB-231 cells (cell density:  $5 \times 10^6$  / 200  $\mu$ L PBS) were injected into the breast fat pad of each mouse. On day 3 after inoculation, the tumor size was measured using digital callipers. After 4 days of inoculation, animals were randomly divided into four groups (n=5): vehicle group, 10-G group (40mg/kg), paclitaxel group (10mg/kg), and paclitaxel (10mg/kg)+10-G group (40mg/kg), according to tumor size as previously described by Schvarcz et al<sup>25</sup> Random numbers were generated using the standard = RAND() function in Microsoft Excel. The vehicle group was given 0.5% CMC-NA carrier and normal saline intragastric administration. 10-G with 0.5% sodium carboxymethyl cellulose (CMC)-Na mixed solution was orally administered once a day. Paclitaxel was diluted with normal saline and administered every 3 days. Body weight was also recorded throughout the trial period. The primary tumor growth was monitored using callipers every 3 days [tumor volume = (length  $\times$  width<sup>2</sup>) / 2]. Thirty-three days post tumor cell injection, the mice were euthanized by carbon dioxide overdose followed by cervical dislocation. The weight of the tumor, liver, and kidney were recorded at the moment of euthanization. The liver and kidney index of mice was

**Table 1** The shRNA Sequence of Lentiviruses

NO.	Target Sequences
Control-shRNA	TTCTCCGAACGTGTACAGT
ADRB2-shRNA	GCCATTA CTTACCTTTCAAG

calculated as follows: Liver coefficient = (liver mass/body weight)  $\times$  100%; Kidney coefficient = (kidney mass/body weight)  $\times$  100%. Body weight, liver and kidney index were an assessment of drug toxicity.

## Immunohistochemistry and TUNEL Analysis

Tumor specimens were immobilized in 4% paraformaldehyde solution for 24 h, followed by standard tissue treatment and embedding. Sections of paraffin-embedded tumor specimens were cut at 4  $\mu$ m and dried overnight at 37°C, dewaxed in xylene twice for 10 min each, and rehydrated with graded series of ethanol. Immunohistochemical staining in the study was done as previously described.<sup>26</sup> The concentrations of primary antibodies: Bcl-2 (1:500), Bax (1:200); cleaved-PARP (1:100), ADRB2 (1:200), phospho-ERK1/2 (1:1000) and Ki67 (1:100). All other chemicals and reagents used in immunohistochemical staining experiments had the highest purity grades available on the market. The results were observed under 10 $\times$  magnifications light microscope (Olympus, BX51) to investigate the expressions in the tumor tissues of the mice. For immunohistochemical quantification, images of three randomly selected microscopic fields per slide were evaluated by independent pathologists.

TUNEL analysis was performed using the method by Zheng et al.<sup>27</sup> Tumor sections were dewaxed and treated with protease K (Beyotime, Jiangsu, China) at 37°C for 30 min to strip proteins from the nucleus. TUNEL detection liquid (Beyotime, Jiangsu, China) was added to the sections and incubated at 37°C for 1 h. After washing with PBS, DAPI (Beyotime, Jiangsu, China) was added to the sections at room temperature for 5 min to stain the nucleus. The fluorescence intensity was observed at an excitation wavelength of 450–500 nm and an emission wavelength of 515–565 nm (Olympus, BX51).

## Haematoxylin and Eosin Staining

All specimens were fixed in 4% paraformaldehyde solution for 24 h, embedded in paraffin and processed using standard histological processing techniques. Serial issue sections (4- $\mu$ m thick) were obtained from each sample, and the H&E results were observed under 10 $\times$  magnifications light microscope (Olympus, BX51) to investigate the pathologic structure of the liver and kidney.

## Statistical Analysis

Data obtained were described using mean (standard deviation), median (range), or frequency (percentage). The independent samples *t*-test (normal distribution) or the Mann–Whitney's *U*-test (non-normal distribution) were applied for the comparison between the two groups. The analysis between the three groups was evaluated by one-way ANOVA or Welch's ANOVA. Tukey's test (equal variances assumed), Dunnett's T3 test (equal variances not assumed) or Dunn-Bonferroni post hoc comparison (nonnormal distribution) was used for post hoc comparison. Statistical analyses were conducted using SPSS version 26.0 for Windows (SPSS, Inc.).

## Results

### 10-G Effectively Inhibits TNBC Cells Proliferation and Colony Formation Ability and Increases Drug Sensitivity of TNBC Cells to Paclitaxel

To explore whether 10-G could sensitize TNBC cells to paclitaxel, TNBC cells MDA-MB-231 and SUM-159 were incubated alone with 10-G, paclitaxel, or 10-G with paclitaxel in increasing concentrations for 48 h (Figure 2A). When exposed to 10-G for 48 h, the IC<sub>50</sub> of 10-G in MDA-MB231 and SUM-159 cells were 139.39 and 195.42  $\mu$ M, respectively. The IC<sub>50</sub> of paclitaxel in MDA-MB-231 and SUM-159 cells after being treated for 48 h was 294.70 nM and 336.18 nM, respectively (Table 2). As shown in Figure 2A, 10-G inhibited the proliferation of MDA-MB-231 and SUM-159 in a concentration-dependent manner. Based on the CI analysis, a synergistic effect of 10-G and paclitaxel was observed (Figure 2A, CI<1). 10-G combined with low-dose paclitaxel (100 nM) significantly enhanced the inhibition of cell proliferation (Figure 2C). In addition, in the non-tumor breast epithelial cell MCF-10A, the inhibition of 10-G was low, having an IC<sub>50</sub> of 619.83  $\mu$ M (Table 2 and Figure 2B). Meanwhile, 10-G did not enhance the cytotoxicity of paclitaxel (Figure 2B). To further verify whether 10-G inhibits the proliferation of TNBC cells, a clonogenic assay was

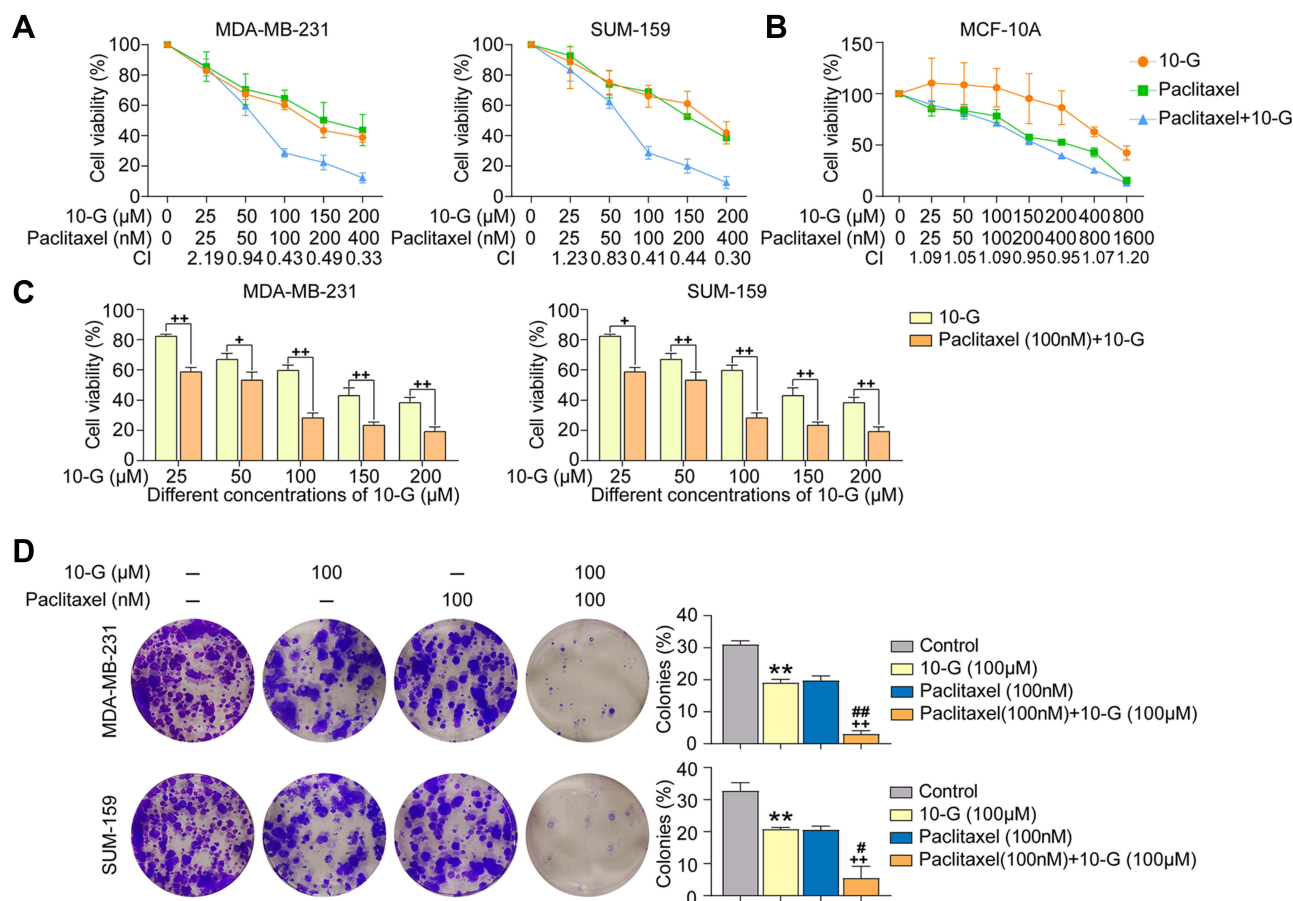


**Figure 2** 10-G synergically inhibited the proliferation and colony formation of TNBC cells with paclitaxel. **(A and B)** TNBC cells MDA-MB-231 and SUM-159, as well as non-tumor breast epithelial cell MCF-10A was treated with different concentrations of 10-G or paclitaxel alone or in combination for 48 h. Cell viability was analyzed by CCK-8 assay. The Combination Index (CI) was calculated with Compusyn software. **(C)** The proliferation of TNBC cells treated with different concentrations of 10-G and combined with paclitaxel (100nM) for 48 h. **(D)** Representative images of colony formation assay in TNBC cells line after drug treatment. Data are represented as the mean value  $\pm$  SD, \*\* $P < 0.01$ , compared with control; ### $P < 0.01$ , compared with paclitaxel; + $P < 0.05$ , ++ $P < 0.01$ , compared with 10-G.

**Abbreviations:** 10-G, 10-gingerol; TNBC, triple-negative breast cancer.

performed with 10-G (100 μM) and/or paclitaxel (100 nM) (Figure 2D). Consistent with CCK8 results, the ability for colony formation was suppressed after drug intervention (Figure 2D,  $P < 0.05$ ). The number of clones in the co-treatment group was significantly lower than that in the monotherapy group (Figure 2D,  $P < 0.05$ ). These results indicate that 10-G could suppress the proliferation of TNBC cells in a concentration-dependent manner and could increase the sensitivity of TNBC cells to paclitaxel.

**Table 2** The Drug IC50 Value of MDA-MB-231, SUM-159 and MCF-10A Cells Treated with Different Concentrations of 10-G or Paclitaxel for 48 h

Cell	Drug IC50	
	10-G (μM)	Taxol (nM)
MDA-MB-231	139.39 (124.65–154.13)	294.70 (182.38–407.02)
SUM-159	195.42 (152.25–238.59)	336.18 (265.47–406.89)
MCF-10A	619.83 (477.21–762.44)	471.12 (377.03–565.21)

**Abbreviations:** TNBC, triple-negative breast cancer; 10-G, 10-gingerol; CCK8, cell counting kit 8; GPCRs, G protein-coupled receptor; CI, combined index; IC50, The half-maximal [50%] inhibitory concentration.

## 10-G Synergistically Promotes Paclitaxel-Induced Apoptosis

Based on the inhibitory effect and chemotherapy sensitization of 10-G on TNBC cells, there was a need to determine whether 10-G inhibited cell proliferation by inducing apoptosis. We exposed MDA-MB-231 and SUM-159 to different concentrations of 10-G and/or paclitaxel for 48 h and studied their apoptosis levels by flow cytometry. The results showed that 10-G significantly promoted the apoptosis of TNBC cells in a dose-dependent manner (Figure 3A and B,  $P < 0.05$ ). The combination of 10-G and paclitaxel significantly increased apoptotic subsets compared to paclitaxel alone (Figure 3A and B,  $P < 0.05$ ). Treatment with 10-G for 48 h was observed to have increased the expression of Bax and cleaved-PARP and decreased the level of Bcl-2 (Figure 3C and D,  $P < 0.05$ ). After combining with 10-G and paclitaxel, the changes of Bax, cleaved-PARP, and Bcl-2 were more obvious (Figure 3C and D,  $P < 0.05$ ). These results suggest that 10-G assists paclitaxel in triggering mitochondrial apoptosis pathways in TNBC cells.

## 10-G Targeting ADRB2 Can Inhibit Cancer and Sensitize Chemotherapy

The interaction between 10-G and ADRB2 through molecular docking was explored to determine whether ADRB2 is a key target of 10-G mediated chemical sensitization. The results showed that the binding energy of 10-G and ADRB2 was 7.7kcal/mol. It was also observed that 10-G docked with the active site of ADRB2. 10-G was closely bound with ADRB2 by forming H-bonds (TYR-316, ASN-312 and SER-203) and hydrophobic contacts (TRP-313, PHE-290, VAL-114 and VAL-117) (Figure 4A). Two lentivirus-delivered vectors were further constructed: ADRB2 shRNA and control shRNA and were transfected into MDA-MB-231 and SUM-159 (Figure 4A). CCK8 and colony assay showed the proliferation and colonies were inhibited after the knockdown of ADRB2 (Figure 4B and C,  $P < 0.05$ ). The tumor inhibition and chemotherapy sensitization of 10-G were, however, weakened (Figure 4B and C,  $P < 0.05$ ). These data suggest that ADRB2 is a major molecular target of 10-G mediated chemical sensitization.

## 10-G Enhanced the Anticancer Effect of Paclitaxel by Inhibiting the Activation of ADRB2/ERK

ADRB2 is considered an upstream regulatory molecule of ERK. Abnormal activation of ERK mediated by ADRB2 plays a key role in tumorigenesis and drug resistance.<sup>28</sup> To determine the regulatory relationship between ADRB2 and p-ERK1/2 in TNBC cells, the levels of ERK and p-ERK1/2 between ADRB2 shRNA and control shRNA were analyzed. Western blotting analysis showed that ADRB2 knockdown inhibited the activation of p-ERK1/2 (Figure 5A and B,  $P < 0.05$ ). The changes in ADRB2, ERK, and p-ERK1/2 expression after 10-G and/or paclitaxel treatment were tested through Western blotting (Figure 5C). It was observed that 10-G inhibited the expression of ADRB2 and p-ERK1/2 proteins in a concentration-dependent manner in MDA-MB-231 and SUM-159 (Figure 5D,  $P < 0.05$ ). After combined treatment with 10-G and paclitaxel, the levels of ADRB2 and p-ERK1/2 were further reduced (Figure 5D,  $P < 0.05$ ). These results suggest that 10-G enhances the inhibitory effect of paclitaxel on TNBC by inhibiting ADRB2/ERK signal.

## 10-G Potentiates the Anti-Tumor Effects of Paclitaxel in a TNBC Xenograft Model

To test the anti-tumor potential of 10-G and paclitaxel either independently or jointly in vivo, MDA-MB-231 cells were subcutaneously injected into NOD/SCID mouse mammary glands to establish a TNBC xenograft tumor model. Based on our pre-experiment on subcutaneous xenograft models, a 40 mg/kg dose of 10-G was administered orally to tumor-bearing mice. Compared with the vehicle group, the 10-G or paclitaxel monotherapy group showed significant tumor growth inhibition (Figure 6A and B). The effect of tumor inhibition was more obvious in the co-treatment group (Figure 6A and B). The test of TUNEL and apoptosis-related protein (cleaved-PARP, Bax and Bcl-2) showed that 10-G and/or paclitaxel significantly increased the apoptosis rate of TNBC (Figure 6C). Correspondingly, compared with the vehicle group, both 10-G and paclitaxel alone had obvious inhibitory effects on the expression of Ki67, and the combined effect of these two compounds was significantly more effective (Figure 6C). From these results, a combination of 10-G and paclitaxel could activate the apoptotic cascade and restrict proliferation in tumor tissues, which then leads to a slowdown of tumor growth. Immunohistochemical results showed that 10-G significantly reduced the expression of ADRB2 and p-ERK1/2 (Figure 6C). When combined with paclitaxel, the expression of ADRB2 and p-ERK1/2 was further reduced (Figure 6C). This was consistent with in vitro.

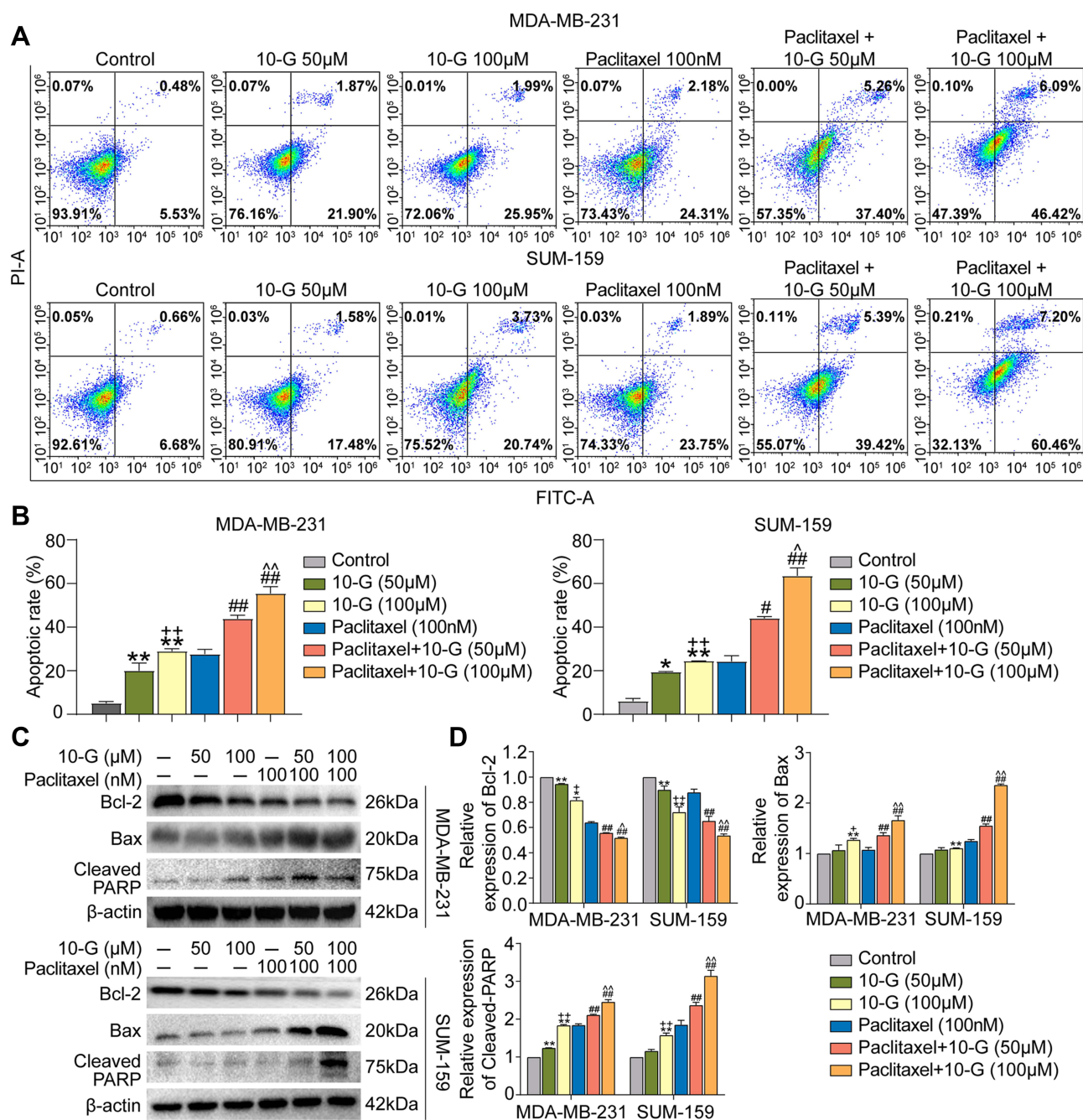


**Figure 3** 10-G induced the cell apoptosis of TNBC cells with paclitaxel. **(A)** MDA-MB-231 and SUM-159 were treated for 24h with 10-G and Paclitaxel alone or in combination, and the level of apoptosis was evaluated using the AnnexinV-FITC/PI dual-labelling technique. **(B)** The apoptotic rate of MDA-MB-231 and SUM-159. **(C and D)** MDA-MB-231 and SUM-159 were treated for 24h with 10-G and paclitaxel alone or in combination, and the protein expression of Bcl-2, Bax and cleaved PARP were detected by Western blot. Data are represented as the mean value  $\pm$  SD. \* $P$ <0.05, \*\* $P$ <0.01, compared with control; + $P$ <0.05, ++ $P$ <0.01, compared with 10-G (50 $\mu$ M); ## $P$ <0.05, ### $P$ <0.01, compared with paclitaxel; ^ $P$ <0.05, ^^ $P$ <0.01, compared with paclitaxel + 10-G (50 $\mu$ M).

**Abbreviations:** 10-G, 10-gingerol; TNBC, triple-negative breast cancer.

## Toxicity Evaluation

As shown in [Figure S1](#), 10-G treatment for 30 days did not result in significant weight loss, while mice treated with paclitaxel alone experienced slight weight loss. The weight loss was not exacerbated in the combination of paclitaxel +10-G versus paclitaxel alone ([Figure 5B](#)). During treatment, the mice did not show adverse effects such as skin ulcers, diarrhea, or death from poisoning. The toxicity of 10-G to the liver and kidney of the mice was further evaluated by H&E staining analysis. No pathologic changes in morphology were observed between the 10-G and

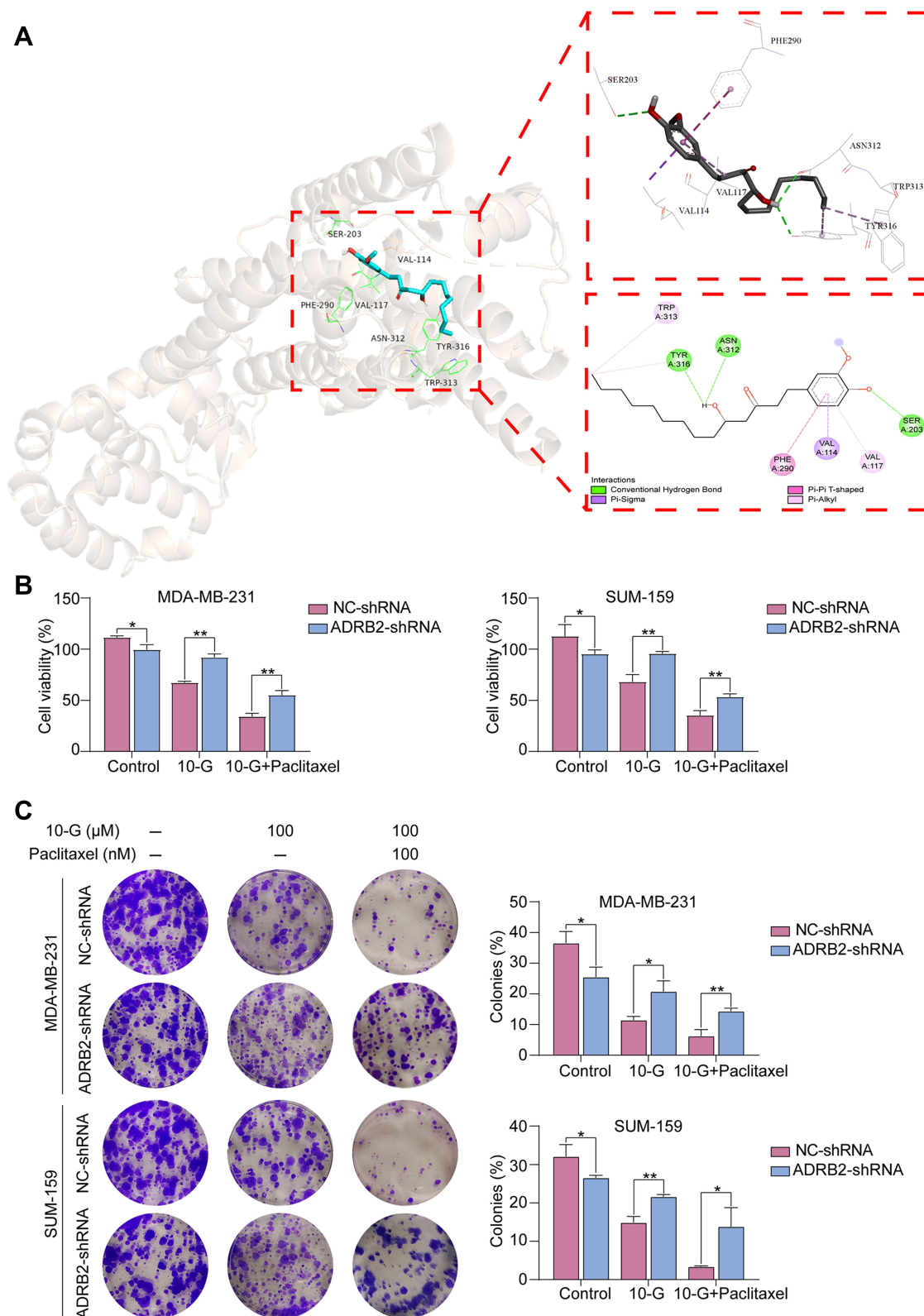


**Figure 4** ADRB2 protein is a key target of 10-G action. **(A)** Ligand interaction and binding diagrams of 10-G at ADRB2 active site. **(B)** MDA-MB-231 and SUM-159 cells were transfected with either NC or ADRB2 lentivirus-shRNA for 48 h, and then were treated with different concentrations of 10-G or paclitaxel in combination for 48 h. The cell viability was determined using CCK-8 assay. **(C)** Targeting of ADRB2 with ADRB2 lentivirus-shRNA transfection inhibited the colony formation ability of TNBC cells MDA-MB-231 and SUM-159, and attenuated the cytotoxicity of 10-G induced TNBC cells. Data are represented as the mean value  $\pm$  SD. \* $P < 0.05$ , \*\* $P < 0.01$ , compared with NC-shRNA.

**Abbreviations:** 10-G, 10-gingerol; TNBC, triple-negative breast cancer.

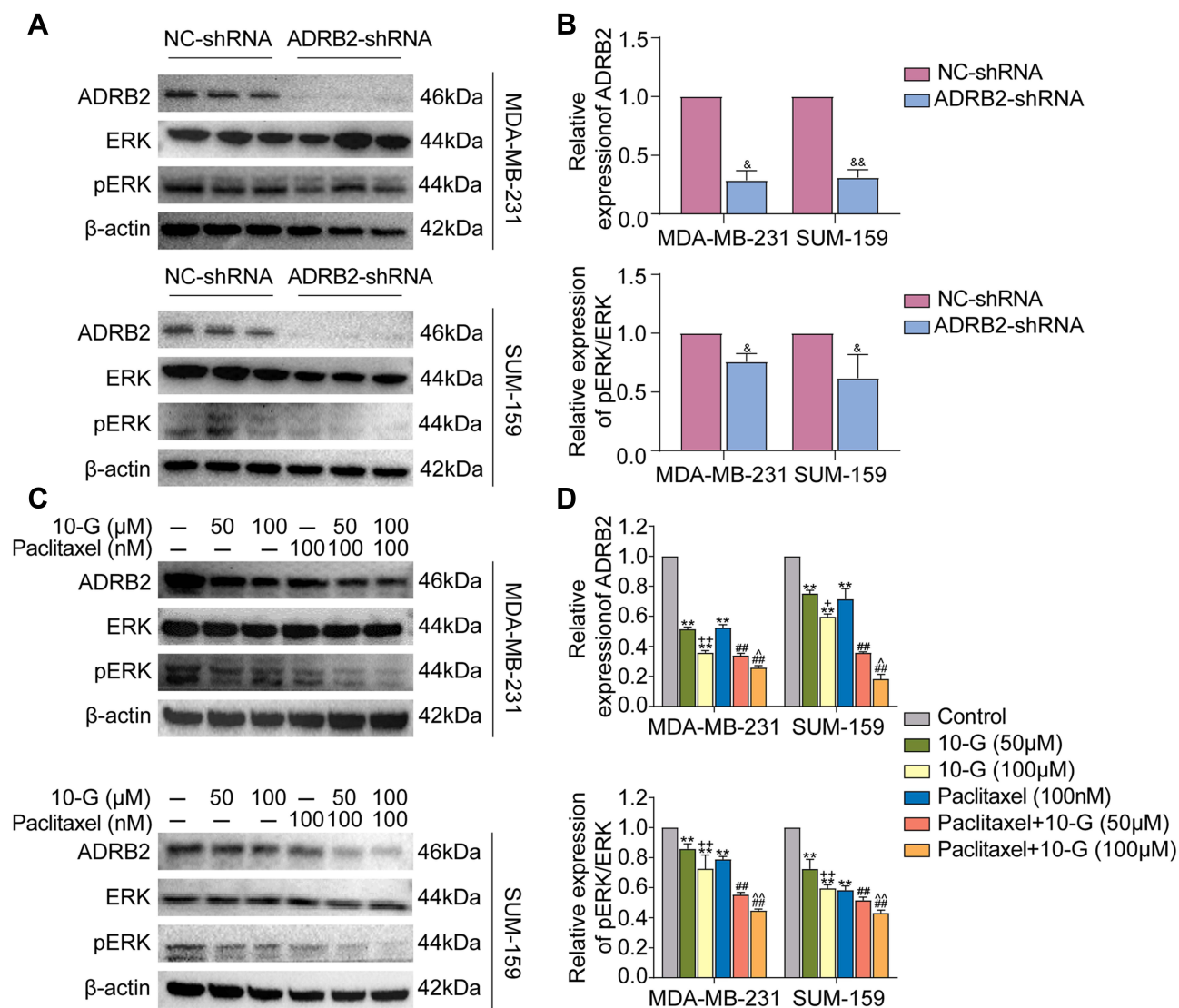


**Figure 5** 10-G interacts with paclitaxel to inhibit ADRB2/ERK signal. (A and B) The protein levels of total ERK and phosphorylated ERK after ADRB2 downregulated by lentivirus-shRNA. (C and D) MDA-MB-231 and SUM-159 were treated for 24h with 10-G and paclitaxel alone or in combination, and the protein expression of ADRB2, total ERK and phosphorylated ERK were examined by Western blot. Data are represented as the mean value  $\pm$  SD. &P<0.05, &&P<0.01, compared with NC-shRNA; \*\*P<0.01, compared with control; +P<0.05, ++P<0.01, compared with 10-G (50μM); ##P<0.01, compared with Paclitaxel; ^P<0.05, ^^P<0.01, compared with Paclitaxel + 10-G (50μM).

**Abbreviations:** 10-G, 10-gingerol; TNBC, triple-negative breast cancer.

vehicle groups (Figure 7A and B). Moreover, there was no significant difference in liver and kidney indices between groups (Figure 7A and B). This reveals that 10-G has good safety in vivo.

## Discussion

TNBC is a highly malignant tumor with considerable potential for metastasis. Chemotherapy is the most widely preferred therapy for THBC. However, long-term use of paclitaxel is often associated with the development of resistance and recurrence. The combination of multiple synergistic agents to reduce the dose of chemotherapy drugs could reduce or slow down the development of single-drug resistance or side effects, and this is considered a promising method for improving the clinical efficacy of cancer treatment.<sup>29</sup> 10-G is considered a potential therapeutic agent because of its inhibitory effects on inflammation and carcinogenesis.<sup>30,31</sup> This study demonstrates that 10-G could increase TNBC cell sensitivity to paclitaxel. Meanwhile, the effective target and the underlying molecular mechanisms of 10-G were uncovered.

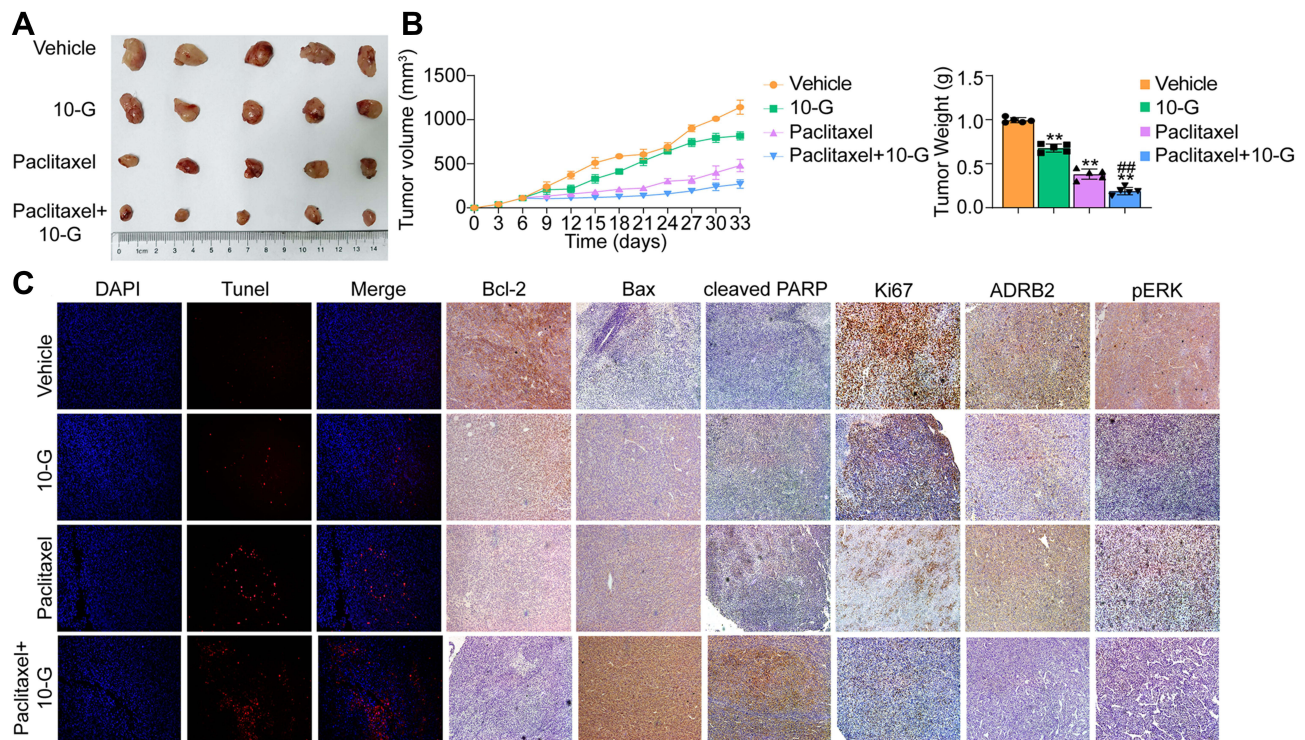


**Figure 6** 10-G enhanced the anti-tumour effect of paclitaxel in vivo. **(A)** Representative tumor image in each treatment group (n=5). **(B)** Tumor volume and tumor weight was measured every 3 days (n=5). **(C)** Representative tumor image of DAPI/TUNEL double-labeling assay of apoptotic cells in each treatment group (n=5). **(D)** The protein levels including Ki67, ADRB2, phosphorylated ERK, Bcl-2, Bax and cleaved PARP was assessed by immunohistochemistry (n=5). Data are represented as the mean value  $\pm$  SD. \*\* $P < 0.01$ , compared with vehicle; ## $P < 0.01$ , compared with Paclitaxel. (magnification,  $\times 100$ ).

**Abbreviation:** 10-G, 10-gingerol.

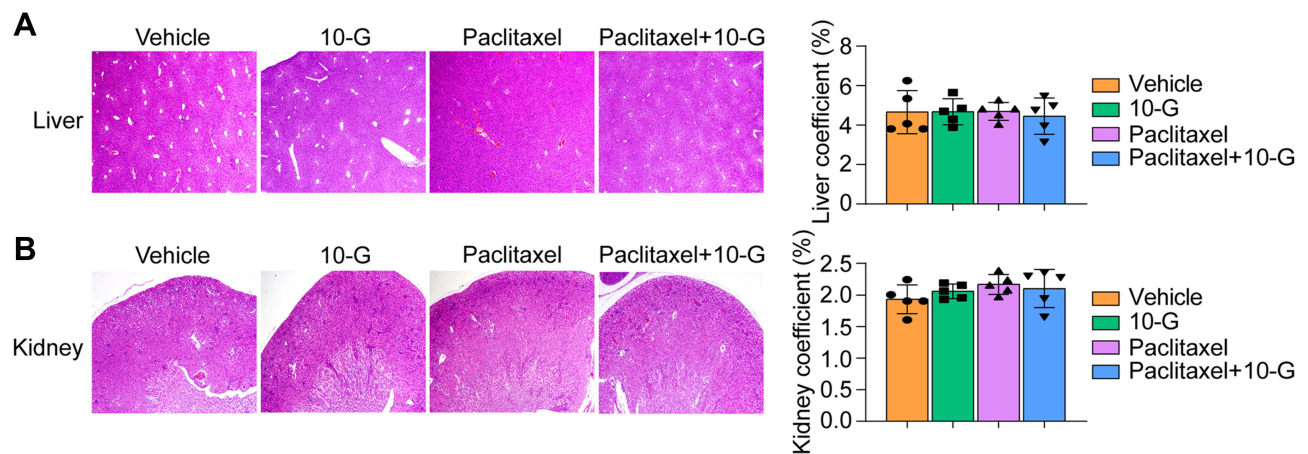


**Figure 7** 10-G did not cause obvious pathologic abnormalities in liver and kidney. **(A)** Representative liver image of H&E staining and liver coefficient in each treatment group. **(B)** Representative liver image of H&E staining and kidney coefficient in each treatment group. Data are represented as the mean value  $\pm$  SD. (magnification,  $\times 100$ ).

**Abbreviation:** 10-G, 10-gingerol.

Apoptosis is a significant step in the eradication of cancer in vivo. It has been reported that 10-G can stimulate the apoptosis of breast cancer cells.<sup>32</sup> The results reported in that study are consistent with this study. Ex vivo results obtained demonstrated that 10-G induces apoptosis and growth inhibition of TNBC cells in a dose-dependent manner. Again, this effect was particularly over-represented with 10-G and paclitaxel combined. These results confirmed that the anti-tumor and chemo-sensitizing effects of 10-G were related to the induction of apoptosis in TNBC cells.

In previous studies, ADRB2 was screened as the first three proteins binding to 10-G by network pharmacology and bioinformatics analysis.<sup>15</sup> It was also confirmed that the interaction between 10-G and ADRB2 was through molecular docking. Both in vivo and in vitro experiments showed that 10-G dose-dependently inhibits the expression of ADRB2. Meanwhile, changes in ADRB2 protein levels were found to be associated with 10-G induced cytotoxicity. ADRB2 knockdown could inhibit the growth and colony formation ability of TNBC cells. This supports the notion that ADRB2 may be a binding target mediating the effect of 10-G. Notably, paclitaxel also reduced the expression of ADRB2, although the antitumor effect of paclitaxel was not weakened after the deletion of ADRB2. Clinical studies have also shown that ADRB2 blocker in combination with paclitaxel does not reduce the efficacy of paclitaxel or increase patients' risk of death.<sup>33</sup> This suggests that ADRB2 is not a binding target for paclitaxel. Targeting ADRB2 may be a new strategy for improving the efficacy of chemotherapy.

In addition, ADRB2 regulates the transduction of several signaling molecules, including the ERK signaling pathway.<sup>34,35</sup> ERK signaling pathway affected cell proliferation, apoptosis, and survival, classically involved in the progression and resistance to chemotherapy of many cancers.<sup>36–38</sup> Phosphorylation of ERK is essential for ERK signaling pathway function, which could promote the development of breast cancer.<sup>39</sup> A study by Xie et al<sup>40</sup> demonstrated that the inhibition of ADRB2 led to a decreased phosphorylation of ERK that provoked growth inhibition and apoptosis in TNBC cells. Here, we also found that ADRB2 knockdown could block ERK phosphorylation in TNBC cells. Recent findings indicate that reducing p-ERK1/2 may improve the treatment efficacy of paclitaxel-based chemotherapy in breast cancer.<sup>41,42</sup> These evidences supported that regulating the activity of ADRB2/ERK signaling might be a potential pathway for TNBC treatment. In this regard, changes in ERK signaling under exposure to 10-G with or without paclitaxel were assessed. Results indicated that the phosphorylation of ERK was reduced by a combination of 10-G and paclitaxel in TNBC, with a dose-dependent inhibitory effect. According to Ryu et al,<sup>43</sup> 10-G could induce mitochondrial apoptosis of colon cancer cells by inhibiting ERK phosphorylation. The chemosensitization of 10-G is therefore closely related to its inhibition of the ADRB2/ERK signaling pathway.

These results further suggest that via targeting ADRB2, 10-G further repressed ERK signaling, restrained growth and enhanced sensitivity to paclitaxel in TNBC. In vivo animal studies further confirmed the obtained in vitro findings and validated the efficacy and safety of 10-G in animal models of breast cancer xenotransplantation.

## Conclusion

In summary, this study suggests that 10-G enhances the chemotherapy sensitivity of TNBC to paclitaxel and that it is related to the ADRB2/ERK signaling pathway. These findings not only highlight that 10-G is a potent anti-tumor agent and a synergist of chemotherapeutic agents in TNBC but also provide new clues for the development of ADRB2-targeted drugs from less toxic natural compounds. In the future, it is required to analyse the effect of 10-G applicable to different groups of TNBC patients.

## Data Sharing Statement

The datasets used and analysed during the current study are available from the corresponding author on reasonable request.

## Ethics Approval and Consent to Participate

The animal study was reviewed and approved by the Ethics Committee of Guangdong Provincial Hospital of Chinese Medicine (Reference No. 2020031).

## Acknowledgements

We thank Bullet Edits Limited for the linguistic editing and proofreading of the manuscript.

## Author Contributions

All authors made a significant contribution to the work reported, whether that is in the conception, study design, execution, acquisition of data, analysis and interpretation, or in all these areas; took part in drafting, revising or critically

reviewing the article; gave final approval of the version to be published; have agreed on the journal to which the article has been submitted; and agree to be accountable for all aspects of the work.

## Funding

This work was supported by the National Natural Science Foundation of China (No. 81974571) and China Postdoctoral Science Foundation (No.2020M682683) (Sponsor: Qianjun Chen, Hai Lu).

## Disclosure

The authors report no conflicts of interest in this work.

## References

1. Siegel RL, Miller KD, Fuchs HE, Jemal A. Cancer statistics, 2021. *CA*. 2021;71(1):7–33. doi:10.3322/caac.21654
2. Ahmad A. Breast cancer statistics: recent trends. *Adv Exp Med Biol*. 2019;1152:1–7. doi:10.1007/978-3-030-20301-6\_1
3. Song X, Zhou Z, Li H, et al. Pharmacologic suppression of B7-H4 glycosylation restores antitumor immunity in immune-cold breast cancers. *Cancer Discov*. 2020;10(12):1872–1893. doi:10.1158/2159-8290.CD-20-0402
4. Lebert JM, Lester R, Powell E, Seal M, McCarthy J. Advances in the systemic treatment of triple-negative breast cancer. *Curr Oncol*. 2018;25 (Suppl 1):S142–S150. doi:10.3747/co.25.3954
5. Won K-A, Spruck C. Triple-negative breast cancer therapy: current and future perspectives (Review). *Int J Oncol*. 2020;57(6):1245–1261. doi:10.3892/ijo.2020.5135
6. Hu M-H, Wu T-Y, Huang Q, Jin G. New substituted quinoxalines inhibit triple-negative breast cancer by specifically downregulating the c-MYC transcription. *Nucleic Acids Res*. 2019;47(20):10529–10542. doi:10.1093/nar/gkz835
7. Liu RH. Potential synergy of phytochemicals in cancer prevention: mechanism of action. *J Nutr*. 2004;134(12Suppl):3479S–3485S. doi:10.1093/jn/134.12.3479S
8. Pezzani R, Salehi B, Vitalini S, et al. Synergistic effects of plant derivatives and conventional chemotherapeutic agents: an update on the cancer perspective. *Medicina*. 2019;55(4):110. doi:10.3390/medicina55040110
9. Hosseini-Zare MS, Sarhadi M, Zarei M, Thilagavathi R, Selvam C. Synergistic effects of curcumin and its analogs with other bioactive compounds: a comprehensive review. *Eur J Med Chem*. 2021;210:113072. doi:10.1016/j.ejmech.2020.113072
10. Li Y, Li S, Meng X, Gan R-Y, Zhang J-J, Li H-B. Dietary natural products for prevention and treatment of breast cancer. *Nutrients*. 2017;9(7):728. doi:10.3390/nu9070728
11. Yahyazadeh R, Baradaran Rahimi V, Yahyazadeh A, Mohajeri SA, Askari VR. Promising effects of gingerol against toxins: a review article. *Biofactors*. 2021;47(6):885–913. doi:10.1002/biof.1779
12. Zhang F, Thakur K, Hu F, Zhang J-G, Wei Z-J. Cross-talk between 10-gingerol and its anti-cancerous potential: a recent update. *Food Funct*. 2017;8(8):2635–2649. doi:10.1039/C7FO00844A
13. Bernard MM, McConnelly JR, Hoskin DW. [10]-Gingerol, a major phenolic constituent of ginger root, induces cell cycle arrest and apoptosis in triple-negative breast cancer cells. *Exp Mol Pathol*. 2017;102(2):370–376. doi:10.1016/j.yexmp.2017.03.006
14. Baptista Moreno Martin AC, Tomasin R, Luna-Dulcey L, et al. [10]-Gingerol improves doxorubicin anticancer activity and decreases its side effects in triple negative breast cancer models. *Cell Oncol*. 2020;43(5):915–929. doi:10.1007/s13402-020-00539-z
15. Huang P, Zhou P, Liang Y, et al. Exploring the molecular targets and mechanisms of [10]-Gingerol for treating triple-negative breast cancer using bioinformatics approaches, molecular docking, and experiments. *Transl Cancer Res*. 2021;10(11):4680–4693. doi:10.21037/tcr-21-1138
16. Philipp M, Hein L. Adrenergic receptor knockout mice: distinct functions of 9 receptor subtypes. *Pharmacol Ther*. 2004;101(1):65–74. doi:10.1016/j.pharmthera.2003.10.004
17. Mele L, Del Vecchio V, Marampon F, et al.  $\beta$ -AR blockade potentiates MEK1/2 inhibitor effect on HNSCC by regulating the Nrf2-mediated defense mechanism. *Cell Death Dis*. 2020;11(10):850. doi:10.1038/s41419-020-03056-x
18. Du Y, Yan T, Zhou L, Yin W, Lu J. A single-nucleotide polymorphism of the beta 2-adrenergic receptor gene can predict pathological complete response to taxane- and platinum-based neoadjuvant chemotherapy in breast cancer. *Breast Cancer*. 2018;10:201–206. doi:10.2147/BCTT.S189197
19. Kafetzopoulou LE, Boocock DJ, Dhondalay GKR, Powe DG, Ball GR. Biomarker identification in breast cancer: beta-adrenergic receptor signaling and pathways to therapeutic response. *Comput Struct Biotechnol J*. 2013;6:e201303003. doi:10.5936/CSBJ.201303003
20. Barron TI, Connolly RM, Sharp L, Bennett K, Visvanathan K. Beta blockers and breast cancer mortality: a population-based study. *J Clin Oncol*. 2011;29(19):2635–2644. doi:10.1200/JCO.2010.33.5422
21. Haldar R, Shaashua L, Lavon H, et al. Perioperative inhibition of  $\beta$ -adrenergic and COX2 signaling in a clinical trial in breast cancer patients improves tumor Ki-67 expression, serum cytokine levels, and PBMCs transcriptome. *Brain Behav Immun*. 2018;73:294–309. doi:10.1016/j.bbi.2018.05.014
22. Wu F-Q, Fang T, Yu L-X, et al. ADRB2 signaling promotes HCC progression and sorafenib resistance by inhibiting autophagic degradation of HIF1 $\alpha$ . *J Hepatol*. 2016;65(2):314–324. doi:10.1016/j.jhep.2016.04.019
23. Khatua B, El-Kurdi B, Patel K, et al. Adipose saturation reduces lipotoxic systemic inflammation and explains the obesity paradox. *Sci Adv*. 2021;7:5. doi:10.1126/sciadv.abd6449
24. Lee S-O, Li X, Hedrick E, et al. Diindolylmethane analogs bind NR4A1 and are NR4A1 antagonists in colon cancer cells. *Mol Endocrinol*. 2014;28 (10):1729–1739. doi:10.1210/me.2014-1102
25. Schvarcz CA, Danics L, Krenács T, et al. Modulated electro-hyperthermia induces a prominent local stress response and growth inhibition in mouse breast cancer isografts. *Cancers*. 2021;13:7. doi:10.3390/cancers13071744

26. Liang Y, Lv Z, Huang G, et al. Prognostic significance of abnormal matrix collagen remodeling in colorectal cancer based on histologic and bioinformatics analysis. *Oncol Rep.* 2020;44(4):1671–1685. doi:10.3892/or.2020.7729
27. Zheng Y, Dai Y, Liu W, et al. Astragaloside IV enhances taxol chemosensitivity of breast cancer via caveolin-1-targeting oxidant damage. *J Cell Physiol.* 2019;234(4):4277–4290. doi:10.1002/jcp.27196
28. Liu Q-G, Li Y-J, Yao L. Knockdown of AGR2 induces cell apoptosis and reduces chemotherapy resistance of pancreatic cancer cells with the involvement of ERK/AKT axis. *Pancreatology.* 2018;18(6):678–688. doi:10.1016/j.pan.2018.07.003
29. Yakisich JS, Azad N, Venkatadri R, et al. Digitoxin and its synthetic analog MonoD have potent antiproliferative effects on lung cancer cells and potentiate the effects of hydroxyurea and paclitaxel. *Oncol Rep.* 2016;35(2):878–886. doi:10.3892/or.2015.4416
30. Ediriweera MK, Moon JY, Nguyen YT-K, Cho SK. 10-Gingerol targets lipid rafts associated PI3K/Akt signaling in radio-resistant triple negative breast cancer cells. *Molecules.* 2020;25:14. doi:10.3390/molecules25143164
31. Zhang F, Thakur K, Hu F, Zhang J-G, Wei Z-J. 10-Gingerol, a phytochemical derivative from “tongling white ginger”, inhibits cervical cancer: insights into the molecular mechanism and inhibitory targets. *J Agric Food Chem.* 2017;65(10):2089–2099. doi:10.1021/acs.jafc.7b00095
32. Fuzer AM, Martin ACBM, Becceneri AB, da Silva JA, Vieira PC, Cominetti MR. [10]-Gingerol affects multiple metastatic processes and induces apoptosis in MDAMB-231 breast tumor cells. *Anticancer Agents Med Chem.* 2019;19(5):645–654. doi:10.2174/1871520618666181029125607
33. Hopson MB, Lee S, Accordino M, et al. Phase II study of propranolol feasibility with neoadjuvant chemotherapy in patients with newly diagnosed breast cancer. *Breast Cancer Res Treat.* 2021;188(2):427–432. doi:10.1007/s10549-021-06210-x
34. Zhang X, Zhang Y, He Z, et al. Chronic stress promotes gastric cancer progression and metastasis: an essential role for ADRB2. *Cell Death Dis.* 2019;10(11):788. doi:10.1038/s41419-019-2030-2
35. Tang J, Li Z, Lu L, Cho CH.  $\beta$ -Adrenergic system, a backstage manipulator regulating tumour progression and drug target in cancer therapy. *Semin Cancer Biol.* 2013;23(6Pt B):533–542. doi:10.1016/j.semcancer.2013.08.009
36. He Q, Xue S, Tan Y, et al. Dual inhibition of Akt and ERK signaling induces cell senescence in triple-negative breast cancer. *Cancer Lett.* 2019;448:1.
37. Ahmed TA, Adamopoulos C, Karoulia Z, et al. SHP2 drives adaptive resistance to ERK signaling inhibition in molecularly defined subsets of ERK-dependent tumors. *Cell Rep.* 2019;26(1):65–78.e5. doi:10.1016/j.celrep.2018.12.013
38. Zhu S, Xu Y, Wang L, et al. Ceramide kinase mediates intrinsic resistance and inferior response to chemotherapy in triple-negative breast cancer by upregulating Ras/ERK and PI3K/Akt pathways. *Cancer Cell Int.* 2021;21(1):42. doi:10.1186/s12935-020-01735-5
39. Mukherjee B, Tiwari A, Palo A, Pattnaik N, Samantara S, Dixit M. Reduced expression of FRG1 facilitates breast cancer progression via GM-CSF/MEK-ERK axis by abating FRG1 mediated transcriptional repression of GM-CSF. *Cell Death Discov.* 2022;8(1):442. doi:10.1038/s41420-022-01240-w
40. Xie W-Y, He R-H, Zhang J, et al.  $\beta$ -blockers inhibit the viability of breast cancer cells by regulating the ERK/COX-2 signaling pathway and the drug response is affected by ADRB2 single-nucleotide polymorphisms. *Oncol Rep.* 2019;41(1):341–350. doi:10.3892/or.2018.6830
41. Lin H, Hu B, He X, et al. Overcoming Taxol-resistance in A549 cells: a comprehensive strategy of targeting P-gp transporter, AKT/ERK pathways, and cytochrome P450 enzyme CYP1B1 by 4-hydroxyemodin. *Biochem Pharmacol.* 2020;171:113733. doi:10.1016/j.bcp.2019.113733
42. Dong Y, Ma Y, Li X, Wang F, Zhang Y. ERK-peptide-inhibitor-modified ferritin enhanced the therapeutic effects of paclitaxel in cancer cells and spheroids. *Mol Pharm.* 2021;18(9):3365–3377. doi:10.1021/acs.molpharmaceut.1c00303
43. Ryu MJ, Chung HS. [10]-Gingerol induces mitochondrial apoptosis through activation of MAPK pathway in HCT116 human colon cancer cells. *In Vitro Cell Dev Biol Anim.* 2015;51(1):92–101. doi:10.1007/s11626-014-9806-6

## Drug Design, Development and Therapy

Dovepress

### Publish your work in this journal

Drug Design, Development and Therapy is an international, peer-reviewed open-access journal that spans the spectrum of drug design and development through to clinical applications. Clinical outcomes, patient safety, and programs for the development and effective, safe, and sustained use of medicines are a feature of the journal, which has also been accepted for indexing on PubMed Central. The manuscript management system is completely online and includes a very quick and fair peer-review system, which is all easy to use. Visit <http://www.dovepress.com/testimonials.php> to read real quotes from published authors.

Submit your manuscript here: <https://www.dovepress.com/drug-design-development-and-therapy-journal>